ELSEVIER

Journal of Fluids and Structures 24 (2008) 1006–1020

JOURNAL OF FLUIDS AND STRUCTURES

www.elsevier.com/locate/jfs

The interaction of an asymmetrical localised synthetic jet on a side-supported sphere

N. Findanis*, N.A. Ahmed

School of Mechanical and Manufacturing Engineering, The University of New South Wales, UNSW, Sydney, NSW 2052, Australia

Received 13 June 2006; accepted 2 February 2008
Available online 18 April 2008

Abstract

A localised synthetic jet offers promise of an optimum and cost-effective practical method of delaying separation and promoting reattachment in fluids with solid body interactions. The asymmetric flow that may result from its use may also be beneficial in improving the aerodynamic performance of a lifting body. There are insufficient studies of synthetic jets, particularly on three-dimensional bluff bodies that are more representative of complex flows in real situations. A comprehensive study on an 80 mm diameter sphere designed with localised synthetic jet orifices was, therefore, conducted in an 18 in × 18 in open circuit closed test-section wind tunnel at a Reynolds number of 5×10^4. The coefficient of pressure distribution was measured by continuously varying the location of the synthetic jet and compared with the no synthetic jet condition. The three-dimensional effects on the flow over the sphere body are particularly made apparent through the growth and the effects of the boundary layer and the deviation from potential flow. Overall, the synthetic jet had the effect of delaying the separation point and extending it further downstream on the sphere surface concomitantly producing a significant reduction in drag, providing solid support to the viability of strategically located synthetic jet when higher lift or lower drag is desired. A surprising discovery was the ability of the synthetic jet to improve the flow at the junction of the sting support and sphere. This has promising implications in devising methods to reduce interference drag that are common in many practical applications such as near junctions between wing and the fuselage.

Keywords: Localised synthetic jet; Three-dimensional; Flow separation; Boundary-layer; Surface pressure distribution; Drag

1. Introduction

The interaction of solid bodies designed with synthetic jet actuators with different types of fluid flows has been of increasing interest in fluid mechanics (Gogineni et al., 2003; Gorder, 2004; Mittal and Rampunggoon, 2002). A testament to this is the ubiquitous nature of vortices and their influence in fluid dynamic theory (Saffman, 1992), synthetic jets being a case in hand that gives rise to vortical type flow. The relentless search for the perfect vortex gives promise for optimised technologies in a variety of engineering applications, in particular to an improved interaction of the flow of fluids with solid bodies. Vortex rings generated by ejecting a pulse of fluid through an orifice optimised for vortex growth gives rise to alternative propulsion systems (Gorder, 2004). Other applications of the synthetic jet include

*Corresponding author. Tel.: +61 2 9385 6721; fax: +61 2 9663 1222.
E-mail address: n.findanis@student.unsw.edu.au (N. Findanis).

0889-9746/$ - see front matter
doi:10.1016/j.jfluidstructs.2008.02.002

Nomenclature

C_d	coefficient of sectional drag
C_p	surface static pressure coefficient $= (p - p_\infty)/(\frac{1}{2}\rho_\infty U_\infty^2)$
C_{pn}	surface static pressure coefficient of port $n = (p_n - p_\infty)/(\frac{1}{2}\rho_\infty U_\infty^2)$
D	diameter of the sphere (mm)
f	frequency (Hz)
O_{P_n}	centre of circle circumscribed by port n, where $n = 1, 2, 3, 4, 5, 6, 7$
O_S	centre of sphere
p	static pressure at a point on the sphere (Pa)
p_∞	freestream static pressure (Pa)
P_n	point on a circle circumscribed by port n
q_∞	freestream dynamic pressure $= \frac{1}{2}\rho_\infty U_\infty^2$ (Pa)
r_n,	radius of a slice centred at O_{Pn} of the sphere circumscribed by port n (mm)
R	radius of the sphere (mm)
Re	Reynolds number $= \rho_\infty U_\infty D/\mu_\infty$
St	Strouhal number, f_D/U_∞
U_∞	freestream velocity (m/s)

Greek Symbols

α	pitch angle (°)
β	yaw angle (°)
γ	port location (°)
θ	angle in general spherical coordinates (°)
μ	absolute viscosity (kg/m/s)
ρ_∞	freestream density (kg/m^3)
ϕ	angle of rotation (°)

flow separation control and turbulence, control of thrust vectoring, augmentation of heat transfer and mixing. Although successful implementation of synthetic jets has been demonstrated in laboratory experimentation (Smith and Glezer, 1998) and in technological advancements (Gogineni et al., 2003), the physical mechanisms by which these modified solid bodies alter the flow field, as well as the gas/aerodynamics of the synthetic jets themselves, have not been fully developed (Mittal and Rampunggoon, 2002). This interaction of the solid body with a synthetic jet and the mean flow of the system can have a significant effect on the flow behaviour of the system (Glezer and Amitay, 2002; Smith and Glezer, 1998). Thus, synthetic jets can provide substantial improvements to the performance of aerodynamic flows by decreasing drag and increasing lift through a transfer of momentum to the flow that delays flow separation and decreases the size of the wake. This is the point of interest of the present paper: considering the interaction of a three-dimensional bluff body with a synthetic jet in a cross-flow.

However, the theories developed to explain the governing dynamics of fluid motion for application to real situations are proving to be difficult (Anderson, 2001; Buresti, 2000). As such, experimental methods are still the main source of physical information for the researcher who is seeking to evaluate the aerodynamic performance of a solid or bluff body (Norberg, 2002).

Although several studies have been conducted on synthetic jet in a cross-flow such as the flow over a circular cylinder (Amitay et al., 1999, 2001; Lee and Goldstein, 2000), there is a noticeable lack of studies on true three-dimensional bodies with synthetic jet (Jeon et al., 2004). The flow over the cylinder can be described with two independent variables and as such is termed axisymmetric. It is a degenerate three-dimensional flow that exhibits certain three-dimensional effects and as such it is neither a really two-dimensional flow nor a fully three-dimensional one. A common phenomenon to all three-dimensional flows is the three-dimensional relieving effect that is present in flow over a sphere but not that of a cylinder; since the flow over a cylinder has in a sense only two ways to travel to get over the body whereas in three dimensions it has an alternative or extra path to travel past and over the body.

In such circumstances, studies on bodies such as spheres are useful in determining the aerodynamic characteristics of these true three-dimensional flows and hence form the basis of the present study (Buresti, 2000).

A striking example of the similarities of the flow over a cylinder and the flow over the sphere is the reduction in drag and the general structure of the wake following the transition from laminar to turbulent flow. There are differences in the flow over a sphere and that of a cylinder quantitatively in the values for the coefficient of drag before and after the transition from laminar to turbulent flow. The sphere shows a reduction in drag from a value of 0.4–0.1, whereas for a cylinder the reduction is from a value of 1–0.3. Similarities are also apparent in the flow-generated instabilities of the cylinder and sphere. These flow instabilities include wake instability (vortex-shedding), separated shear layer instability and boundary layer instability. Boundary-layer instability is a term used to describe disturbances that affect the stability of the boundary layer (Reshotko, 1976). For instance, if the forced disturbance that enters the boundary layer is large enough, then this will cause the boundary layer to transition from laminar to turbulent flow. If the disturbance is small, then it will tend to excite free disturbances or normal modes of the boundary layer that are generally referred to as Tollmien–Schlichting waves.

In some sense, synthetic jets may be considered a time-averaged fluid motion generated by sufficiently strong oscillatory flow at a sudden expansion. A characteristic feature of synthetic jets is that their formation takes place

within the fluid flow. The net mass added is zero, but the synthetic jet energises the flow by imparting linear momentum. The vortex pairs formed progress into turbulence and the monotonic decrease of their streamwise velocity leads to their dissolution.

Synthetic jets may be applied either in a distributed manner or from localised sources; also oscillatory streaming motions can be induced in the fluid acoustically through the transmission of sound or 'acoustic streaming' (Glezer and Amitay, 2002; Jeon et al., 2004). A case in hand is the work of Kim and Durbin (1988) in which a uniform acoustic field is applied symmetrically from a distance to the airflow interacting with the sphere, in the Reynolds number range of $500 < \mathrm{Re} < 60\,000$. The results indicated that, when the acoustic excitation was near to the natural instability of the flow, a decrease in the wake size occurred as a consequence of the separation point being delayed and pushed further downstream towards the wake region. This created a rapidly thickening but broader and shorter recirculation zone from the inwardly directed shear layer. This also produced a lower base pressure behind the sphere and possibly in the near-wake region, with a higher velocity in the recirculation zone as a result of a reduced size of the separation bubble. Since the forcing was being applied away from the body, an increase in the turbulence level with a consequent increase in the base pressure over the body was produced which then resulted in higher drag.

Additionally, experimental investigations carried out by Jeon et al. (2004), on a sphere with a uniform acoustic field emanating from a slot located at an angle of 76° from the fore stagnation point, but equally distributed circumferentially around the sphere, showed that for forcing frequencies equal to or greater than the critical frequency, $\mathrm{St} = 2.85$ or 190 Hz, there was a reduction in drag of nearly 50%. This forcing frequency corresponded to the boundary-layer instability frequency that delayed flow separation and consequently triggered the high shear-layer instability frequency for reattachment of the flow. The boundary-layer instability frequency falls in-between the low wake instability frequency (vortex shedding) and the high shear layer instability frequency, which at this Reynolds number are $\mathrm{St} = 0.18$ and 10, respectively. The boundary-layer instability frequency seems to correspond to the particular frequency that is receptive of disturbances to the normal modes of the boundary-layer or, as mentioned earlier, the Tollmien–Schlichting waves, since laminar separation is maintained. The works of Kim and Durbin (1988) as described above showed that the reverse flow region became stronger and that the total drag was increased with acoustic forcing. Jeon et al. (2004) has suggested that the mechanism for reducing drag at the critical frequency could be due to the corresponding high frequency boundary-layer instability.

The work by Glezer and Amitay (2002) using a synthetic jet placed locally on one side of a cylinder showed a reduction in surface pressure both upstream and downstream of the forcing location. The actuation of the synthetic jet induced a local separation bubble beginning at the location of the synthetic jet and ending at the point of reattachment. This mechanism of drag reduction was referred to as "virtual aero-shaping" (Mittal and Rampunggoon, 2002) which displaces local streamlines well outside the undisturbed boundary-layer and rapidly decreases the upstream and downstream surface pressure of the forcing location. Thus, a delay in separation results from the increased velocity of the potential flow outside the surface boundary-layer which is greater than the velocity of the unforced potential flow. It is not well established as to when or under what conditions these bubbles will form, particularly in three-dimensional flows with the synthetic jet impinging on the cross-flow and forming a recirculation zone.

A rather straightforward and effective way to examine how the aerodynamic behaviour of a bluff body in terms of boundary layer growth, skin friction, separation of flow and pressure drag in three dimensions, under the influence of synthetic jet changes, is to use a sphere, which has a symmetrical shape. The sphere may be manufactured with a fixed synthetic jet orifice and a set of pressure tapping points around it. Designing the experiment in this fashion provides the distinct advantage of being able describe the influence of the synthetic jet on the same set of points on the sphere as it is rotated relative to the free stream.

It is interesting to note that the maximum Reynolds numbers at which Kim and Durbin (1988) and Jeon et al. (2004) conducted their experiments form approximately the two limits of the plateau-like region on the C_D curve for a sphere (Schlichting, 1968) where the drag practically remains unchanged with changes in the Reynolds number. It appears that the effect of a localised synthetic jet on the flow over a sphere at a Reynolds number that lies within those limits would be a suitable choice and the present study was, therefore, conducted at a Reynolds number of 5×10^4.

In summary, the present work seeks to show that a localised synthetic jet can achieve significant aerodynamic improvement on the flow over a three-dimensional bluff body by delaying flow separation and reattachment and reducing drag without triggering flow instability frequencies, but rather through the input of momentum to the flow. Furthermore, that a localised synthetic jet has the ability to modify the flow over a sphere a substantial distance away from the point source in all three dimensions. The asymmetrical location of the synthetic jet on the sphere body will induce these three-dimensional changes, enhancing the effect of localising the synthetic jet as opposed to a distributed or symmetrically located synthetic jet. The asymmetry will also prove useful in relation to the side support of the sphere body and whether it will improve flow around this flow disturbance. This work on the asymmetrical location of a synthetic jet will prove to be most beneficial in generating lift not only on bluff bodies but more importantly on

streamlined lifting bodies. Also of interest is to determine whether the localised synthetic jet will generate a separation bubble such as that observed in other recent applications of distributed synthetic jet.

2. Experimental methods and procedures

The experimental work was conducted using an 18 in × 18 in open circuit, closed test-section, NPL-type wind tunnel at UNSW aerodynamics laboratory (Ahmed and Archer, 2001; Ahmed and Wagner, 2003). The wind tunnel was operated at an air speed of 10 m/s. The bluff body used for the experiments was an aluminium sphere of 80 mm diameter and supported horizontally by a rod attached to one side of the sphere. Using the method of Barlow et al. (1999), the blockage ratio was calculated to be 2.8%. Additional velocity profiles obtained using hot-wire anemometry on the centreline plane of the sphere showed little or no difference from the free-stream velocity profile confirming that tunnel blockage was negligible. The sphere was designed with a synthetic jet orifice (labelled SJ in Fig. 1) of 1 mm diameter and oriented at a 45° tangent to the normal of the sphere surface, and had seven pressure ports on the centreline axis of the sphere (Fig. 1). An electronic scanivalve unit with controller and port indicator and a FCO510 digital manometer were used to measure the pressure. The sphere was rotated to each predetermined angular position with sufficient time allowed for the pressure to settle before a measurement was taken.

The synthetic jet actuator was composed of a modified compressor and a 12 V power supply. The compressor piston was fitted with a one-way valve that was modified to cause suction and blowing as it reciprocated instead of constant compression of the air. The compressor line was connected to the synthetic jet orifice on the sphere using silicon tubing. The sphere support was fitted against a fixed protractor to measure the angle of rotation.

The velocity of the synthetic jet was measured using a Dantec Streamline CTA Anemometer system with a 55P14 probe. The probe was calibrated using the Dantec Flow Calibration System. The voltage supplied to the motor was through a DC power supply unit to generate the desired frequency with a range of 10–75 Hz. The frequency obtained from hot-wire measurement was cross-checked against the rotational speed of the motor using a laser tachometer. The velocity profile corresponding to synthetic jet is shown in Fig. 2. Since the hot-wire measurement is indifferent to flow direction and the two extremes, that is blowing and suction, are 180° out of phase, the peaks are both positive for suction and blowing. The maximum velocity measured was about 35 m/s, and its r.m.s. value was 15 m/s. The actuation frequency was $f = 60$ Hz (Fig. 2) that corresponded to $\mathrm{St} = 0.53$. This value was chosen to avoid correlation with the low wake instability frequency (vortex shedding frequency) and the high instability frequency (separating shear layer instability frequency) which are at $\mathrm{St} = 0.19$ and 6, respectively, at the present Reynolds number. Rather than examining the effect of the synthetic jet as targeted towards flow instabilities, this paper focuses on the mechanism of 'virtual aeroshaping' as a means to control the flow over the sphere and thereby improve aerodynamic performance through a reduction in drag. Work on a two-dimensional body (Glezer and Amitay, 2002) has shown an improvement in the delay of separation for a Strouhal number of 2.5 for a circular cylinder. Whether similar improvement of the flow over three-dimensional flow can be obtained with the application of the localised synthetic jet was, therefore, a major motivation of this project.

Flow visualisation was carried out using tufts (Bradshaw, 1970) to obtain a visual estimate of the flow direction and location of the separation point on the sphere.

3. Results and discussion

3.1. The theoretical coefficient of pressure on the surface of a sphere

An attempt was made to compare the experimental value with the theoretical value of C_p (coefficient of pressure distribution) at each of the tappings for the no-jet condition. With reference to Fig. 3, the static pressure at a point on a sphere (Pisasale and Ahmed, 2002a, b, 2004) is given by

$$p(\theta) = p_\infty + \frac{9}{4} q_\infty \cos^2\theta - \frac{5}{4} q_\infty. \tag{1}$$

Re-arranging the above equation and using the geometrical relation that $\cos\theta = \cos\alpha\cos\beta$ and dividing by the dynamic pressure q_∞, the following expression for C_p was obtained

$$C_{p1,2,\ldots}(\alpha,\beta) = \frac{9}{4}\cos^2\alpha\cos^2\beta - \frac{5}{4}, \tag{2}$$

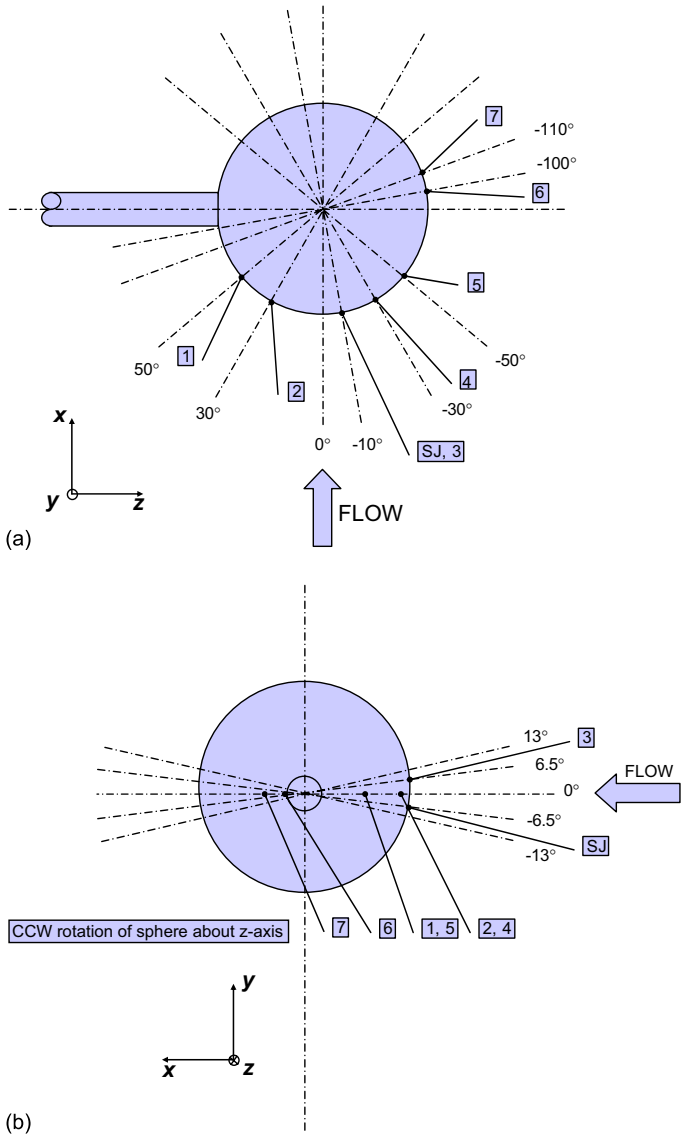

Fig. 1. Schematic diagrams of sphere: (a) plan view (top) and (b) elevation view (bottom).

where

$$\cos^2\alpha = \sin^2\gamma + \cos^2\gamma\cos^2\phi, \quad \cos^2\beta = 1/(A+1) \tag{3,4}$$

in which $A = (\sin^2\gamma)/(\cos^2\gamma\cos^2\phi)$.

Here α was measured from the horizontal centre plane, whereas angles β and γ were measured from the vertical centreline of the sphere. Note that $0^\circ \leqslant \phi \leqslant 180^\circ$, which was the rotation of the sphere about its horizontal axis passing through the sting support or the z-axis. As the sphere was rotated through the range $\phi = 0^\circ$ to $\phi = 180^\circ$ each pressure tapping circumscribed a semicircle and the path of each tapping represented a particular slice through the sphere as it was rotated through ϕ. The variation in pressure coefficient in a two-dimensional sense could thus be examined as a function of ϕ, while in a three-dimensional sense as a function of θ, which was the angular displacement from the stagnation point and was a function of the angles α and β.

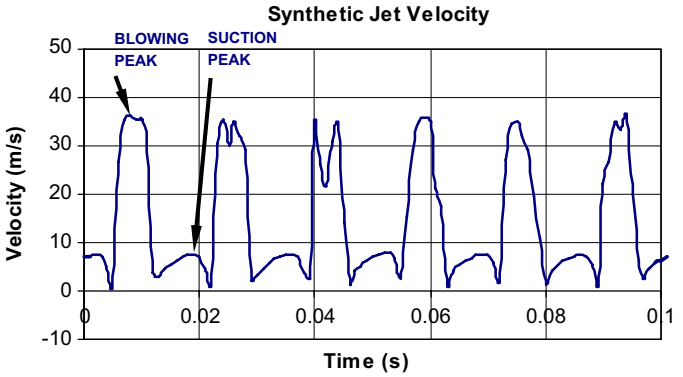

Fig. 2. Hot-wire measurement of synthetic jet flow.

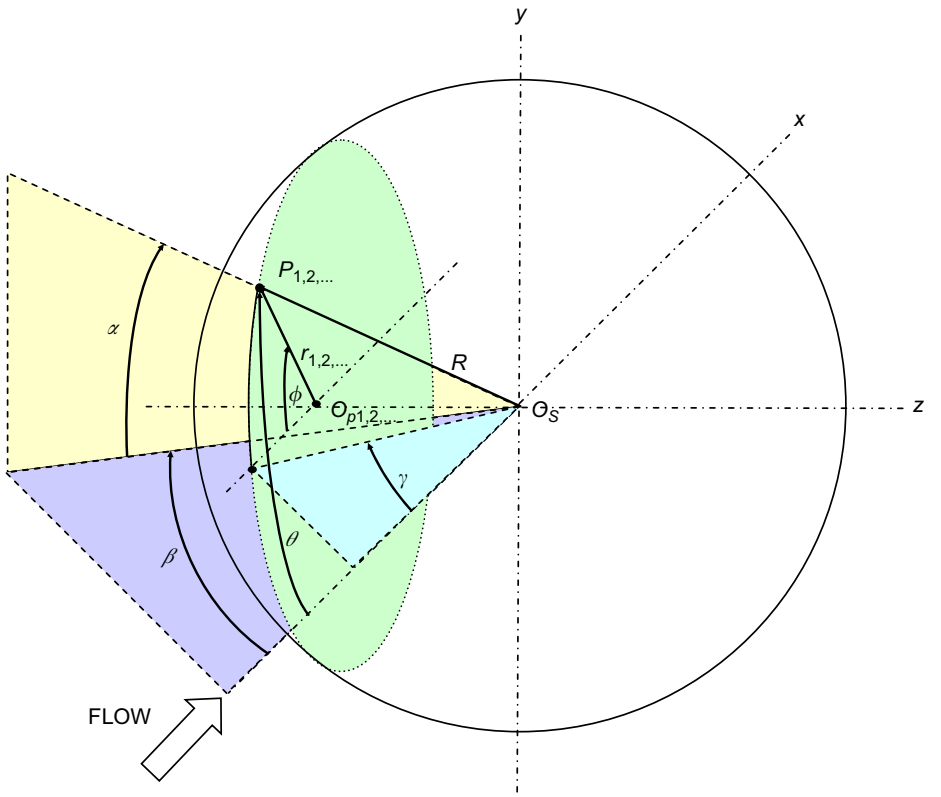

Fig. 3. Analysis of surface pressure on the sphere.

3.2. The two- and three-dimensional effect of the localised synthetic jet

Fig. 4(a) shows the pressure coefficients for pressure tapping or port no. 3. Port 3 is offset 10°, that is, $\gamma = 10^\circ$. The potential flow curve obtained was similar to that of a cylinder with the experimental and theoretical curves at the front stagnation point, coinciding at 0° to the same value. The C_p curve showed good agreement between the experimental results without and with synthetic jet and the potential flow curve at low angles. Notably in Fig. 4(b), the curve began from $\theta = 10^\circ$ since port 3 had a 10° offset to begin with and ended at $\theta = 170^\circ$ for the same reason. This offset applied to all ports with their respective angular offsets. As the sphere was rotated through higher angles of θ the flow began to

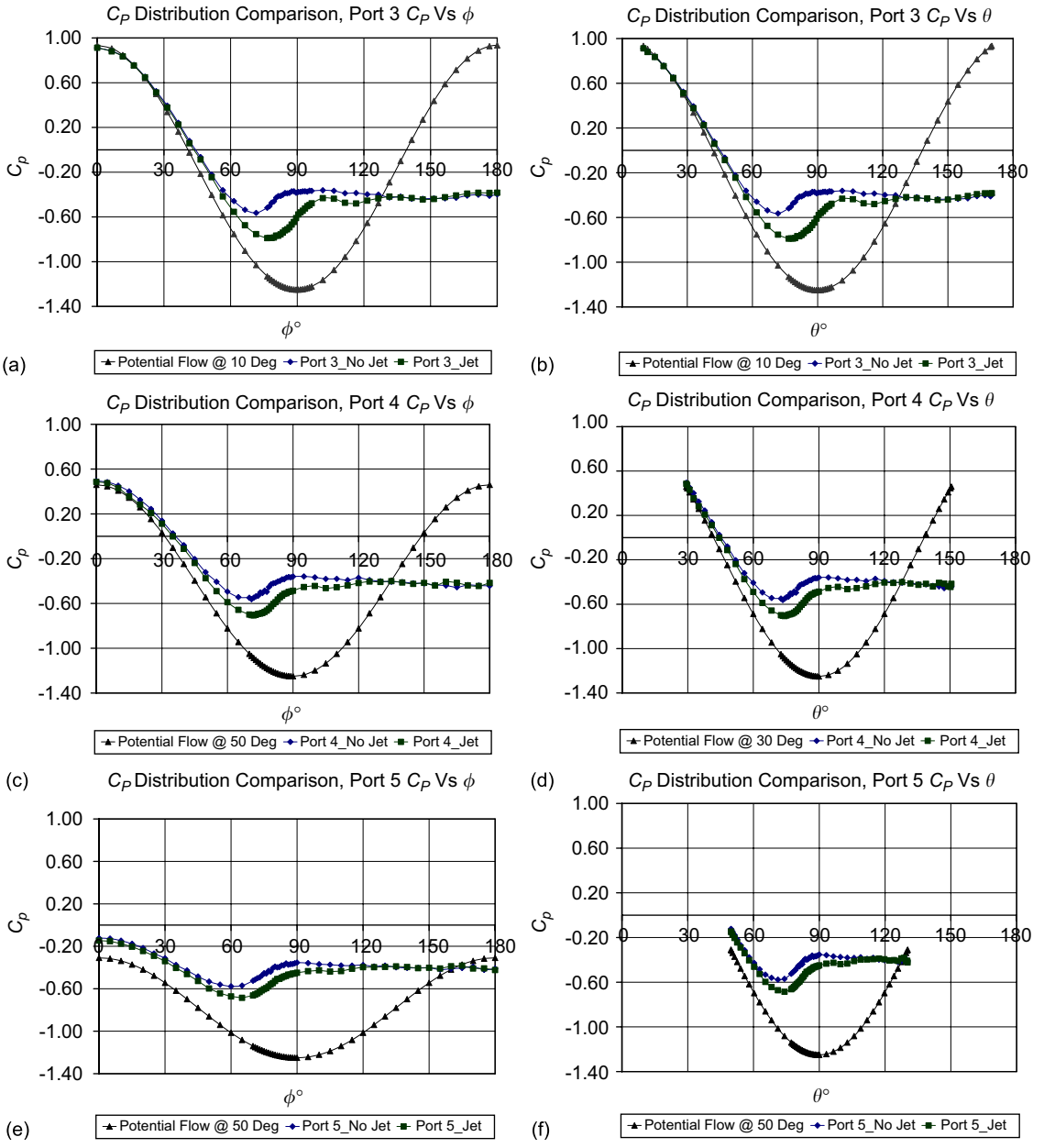

Fig. 4. (a) C_p distribution for port 3 with respect to ϕ; (b) C_p distribution for port 3 with respect to θ; (c) C_p distribution for port 4 with respect to ϕ; (d) C_p distribution for port 4 with respect to θ; (e) C_p distribution for port 5 with respect to ϕ; and (f) C_p distribution for port 5 with respect to θ.

deviate from the potential flow curve at approximately $\theta = 27^\circ$. This is to be expected since the boundary layer is thin near the front stagnation point but gradually thickens and eventually separates (Clift et al., 1978).

Table 1 shows this deviation from potential flow theory. As mentioned above, port 3 is less than 27° offset, and as such does not show any initial deviation from potential flow theory. Ports 1 and 2 do show deviation and more so than their symmetrically opposite pair, ports 5 and 4, respectively, because of the effect of the sting support which will be discussed in more detail. Port 6 and port 7 are very close to flow separation and an escalation of the rate of deviation is observed.

Table 1
Potential flow deviation

Percentage deviation from potential flow		
Port no.	γ	%
1	50	22.0
2	30	20.0
3	−10	0.0
4	−30	3.3
5	−50	10.0
7	−70	20.0
6	−80	32.5

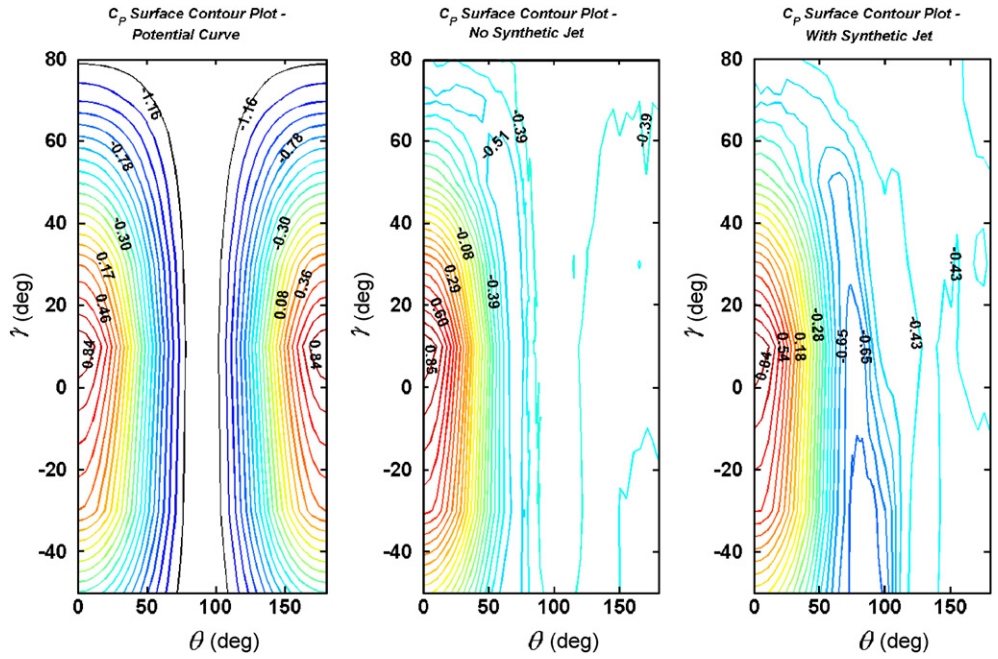

Fig. 5. Surface pressure contour plot of: (a) potential flow, (b) with no synthetic jet; and (c) with synthetic jet.

The synthetic jet begins to influence the flow characteristics over the sphere at $\theta = 17^\circ$ but the deviation is small. The synthetic jet is most effective between $\theta = 45^\circ$ and 130°. It is within this range that the boundary layer grows considerably in size and subsequently causes the build up of an adverse pressure gradient, which induces the reversal of flow that eventually results in flow separation. Thereafter, flow separation enters the wake region of the sphere. When the synthetic jet is in this range of between $\theta = 45^\circ$ and 130° it has the capability to delay flow separation through the input of momentum to the flow and reattach flow already separated in the wake region on a three-dimensional bluff body. Fig. 4(a)–(f) provides the evidence that the effect of the synthetic jet is to delay flow separation and reattach the flow. Every C_p distribution plot in Fig. 4(a)–(f) shows the same trend when the synthetic jet is activated, the surface pressure is altered with a shift towards the potential flow curve. Further to this, Fig. 5 provides even more clarity as to the extension of the separation line with the actuation of the synthetic jet. The first plot in Fig. 5 shows the surface pressure distribution of potential flow theory, with the second plot showing the surface pressure distribution of the sphere with no synthetic jet. Of course, potential flow theory does not show a line of separation, although the line of separation in this second plot would be indicated when the change in surface pressure coefficients becomes almost nil. This happens approximately when the C_p reaches a value of -0.39, corresponding to an angle of $\theta = 83^\circ$. With the activation of the synthetic jet, this value

changes to approximately −0.43, corresponding to a maximum angle of approximately $\theta = 120^\circ$. In addition, Fig. 4(a)–(f) shows subtle evidence of the creation of a separation bubble after which we see reattachment of the flow. The separation bubble would seem to be located at the point on the plots where the synthetic jet curve has a very small plateau-like region. For example, in Fig. 4(b) the separation bubble would be seem to be formed at approximately when $\theta = 81^\circ$. Fig. 4(d) and (f) shows the formation of the separation bubble to be at approximately when $\theta = 86^\circ$. The work of Jeon et al. (2004) also showed the formation of a separation bubble, although since the synthetic jet in that case was distributed around the circumference of the sphere as opposed to a localised synthetic jet in this case, the plateau effect of the separation bubble in the surface pressure distribution was more pronounced. Another possibility as to the formation of the separation bubble could be due to flow transition, as indicated by the Reynolds number of the flow, and thus the synthetic jet was providing momentum to stabilise the bubble according to the published results of Jeon et al. (2004). It is interesting to note that at the critical Reynolds number of about 3.5×10^5 laminar separation occurs at $\theta \simeq 100^\circ$ followed by reattachment at $\theta \simeq 117^\circ$. Finally, turbulent separation occurs at $\theta \simeq 135^\circ$ (Taneda, 1978). In the present work the localised synthetic jet, at a much lower Reynolds number of 5×10^4, provides similar aerodynamic improvement by delaying flow separation up to an angle of $\theta \simeq 130^\circ$.

The results indicate that a localised synthetic jet asymmetrically located on a three-dimensional bluff body has the capability to effect significant changes to the surface pressure distribution before and after flow separation has occurred not only in the local vicinity of the synthetic jet but also at significant distances from the point source. The train of vortices produced by the synthetic jet appear to transfer momentum in all three dimensions to induce global flow improvements. The interaction between the synthetic jet and the cross-flow over the sphere can lead to a local displacement of the cross-flow and thereby induce a "virtual" modification of the flow boundary through the creation of a local separation bubble and therefore alter the local pressure and subsequent vorticity distributions. Further aerodynamic improvement could be attributed to the re-energising of the boundary-layer which would promote more mixing and possibly entrain the nearby higher energy flow into the wake region.

3.3. Flow visualisation study of the effect of the localised synthetic jet

The tufts themselves give evidence of flow separation. Streamlined attached flow is indicated when the tuft is attached to the surface of the sphere and is directed along the contour of the sphere surface, whereas the tuft lifts off the surface of the sphere and moves erratically when flow separation occurs. This can be observed in the photographic image of the tuft indicated by a clear streamlined image for that portion of the tuft before flow separation has occurred, with the remainder of the image of the tuft being noticeably blurred due to the unsteady movement of the tuft as a result of the unsteady flow, thus indicating that the flow has separated. The surface pressure distribution of the sphere without synthetic jet [Fig. 6(a)] indicates that flow separation occurs at an angle of approximately 85° (marked by the black bold line). When the synthetic jet is activated, the separation point was seen to extend by approximately 13° giving a new separation angle of 98° [marked by the bold black line Fig. 6(b)]. This is comparable with the published works of a distributed synthetic jet on a cylinder which was previously examined in the surface pressure distribution results of Fig. 4(e).

The sphere was then rotated further to an angle of 110°. The separation of the tufts occurred from the root of the tufts since the entire length of the tufts are in the separated flow region [Fig. 7(a)] as indicated by the separation line. When the synthetic jet was applied [Fig. 7(b)], the flow was streamlined and the tufts near ports 1 and 2 remained attached for a substantial length. The activation of the synthetic jet had the effect of delaying the separation until approximately 120°, as indicated by the separation line. Not all the tufts leave the surface at the same angle from the stagnation point, that is the separation is not symmetrical around the circumference of the sphere. This visual observation can be confirmed by the C_p plots. The point of separation or the separation angle differs for ports 3, 4 and 5 [Fig. 4(a)–(f)].

3.4. Effect of sting support

By examining closely the C_p distribution figures, an apparent asymmetricity in the experimental results for the pairs of ports that are symmetrically opposite about the centre axis was observed. The results were not similar for ports 1 and 5 and for ports 2 and 4 as was expected, but markedly different for each pair of ports for the two conditions of without synthetic jet and with synthetic jet. The apparent discrepancy was initially speculated to be the effect of the rod support on the nearby ports of 1 and 2. To confirm this, an experiment was conducted that consisted of placing an equivalently sized rod symmetrically opposite to the sting support of the sphere. Pressure measurements from ports 1 and 2 were compared to the results of ports 4 and 5 [Fig. 8(a) and (b)]. When the rod was placed in the flow on the opposite side of the sphere, pressure measurements on both sides of the sphere strongly agreed. This confirmed that the effect of the rod altered the values of the surface pressure on the sphere.

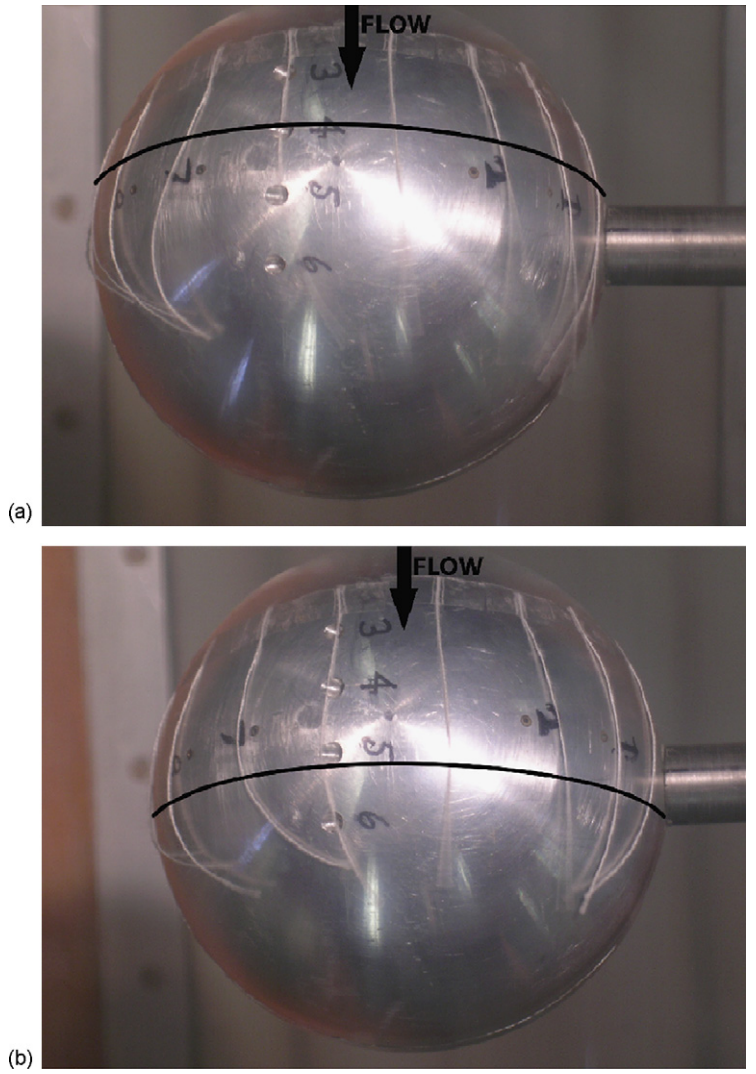

Fig. 6. Sphere rotated 90°: (a) with no synthetic jet and (b) with synthetic jet.

With the condition of an activated synthetic jet, the effect of the localised synthetic jet significantly shifted the pressure distribution for port 1 toward the potential flow curve. The same can be said for port 2 which also shows a high improvement in surface pressure distribution. In fact, after approximately 70° the pressure distribution for port 1 corresponds to that of port 2. This shows the ability of the synthetic jet to correct flow even under the adverse flow conditions generated by the sting support. The sting support disturbs the flow, pushing the pressure distribution further away from potential flow. With the activation of the synthetic jet, an asymmetrically improved flow field is generated that results in a greater improvement to the flow on the sting side of the sphere than the unsupported side of the sphere.

The correction to the flow attributed to the actuation of the synthetic jet, even with the added interference from the sting support, could have significant implications for improvements in aerodynamic applications that seek to reduce interference drag.

3.5. Further remarks on flow separation

Fig. 6(a) shows the sphere rotated through 90°. As mentioned earlier, the flow exhibited some degree of turn in towards the middle of the sphere but did not follow the contour of the sphere completely, since the flow separated and

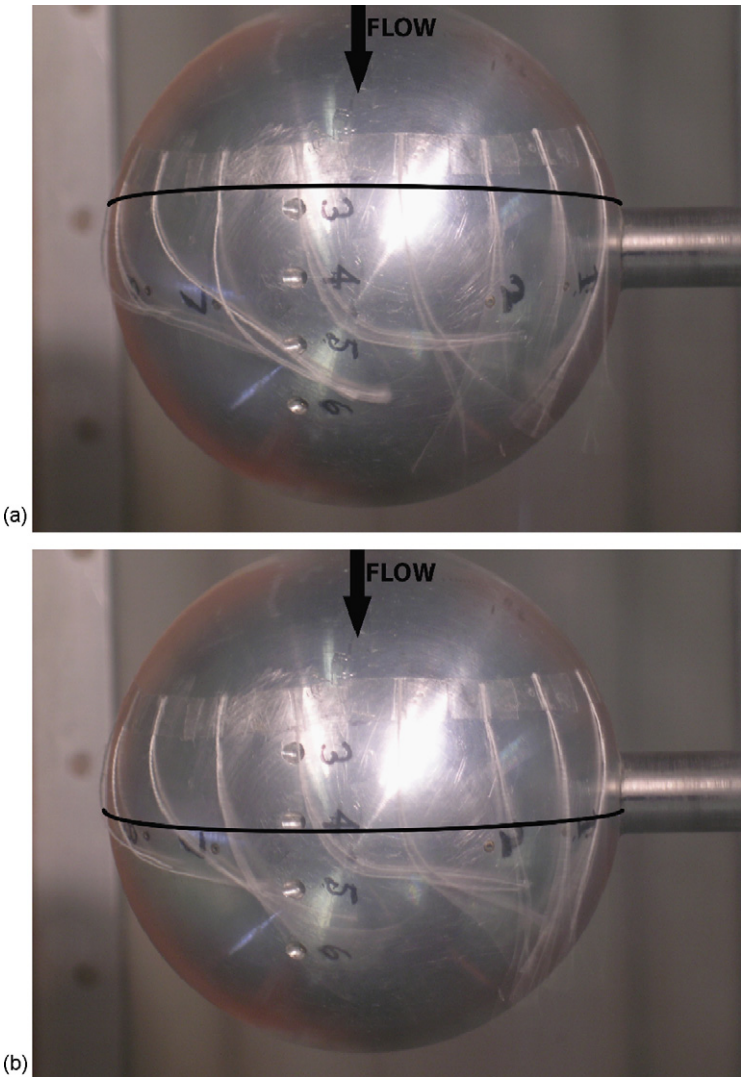

Fig. 7. Sphere rotated 110°: (a) with no synthetic jet and (b) with synthetic jet.

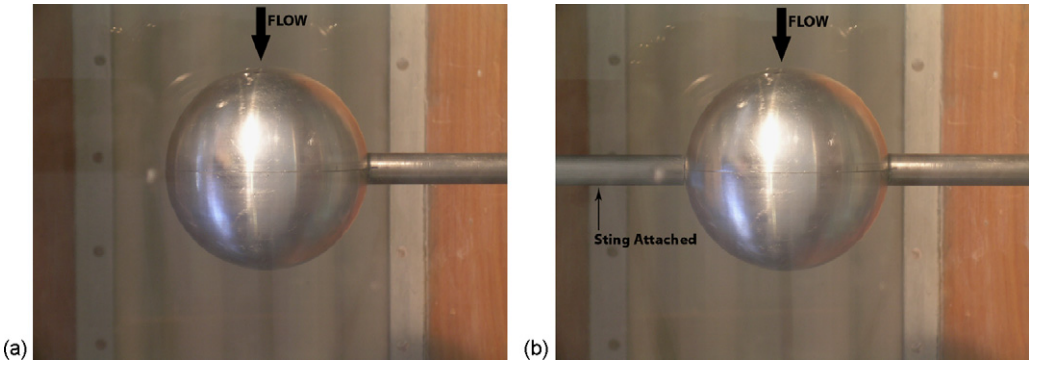

Fig. 8. Sphere plan view: (a) without rod attached and (b) with rod attached.

formed the turbulent wake region. The slight tendency for the flow to be directed from left to right was due to the influence of the sting support on the right. With the activation of the synthetic jet [Fig. 6(b)], the flow showed greater stability, with less erratic movement of the tufts, as well as an improvement in the symmetricity of the flow depicted by the tufts turning in towards the middle on both sides. It was apparent from Fig. 7(a), where the rotation of the sphere was through 110°, that the flow turned in from the left side of the sphere and headed across the sphere towards the right side i.e. the flow was moving from port 5 to port 2. This asymmetrical tendency in the flow was due to the sting support, which at this angle had a greater influence on the flow and seemed to entrain the flow from the opposite side of the sphere. With the activation of the synthetic jet at this angle, this asymmetrical flow was stabilised as the tufts showed less flutter. It was also clear that the tuft to the left of orifice 4 was being forced to straighten due to the synthetic jet [Figs. 6(b) and 7(b)].

Fig. 9 shows a diagrammatic representation of the separation line as viewed top down on the sphere. There are two separation lines shown on the sphere, one without and the other with the application of the synthetic jet. It is immediately apparent that the effect of the synthetic jet was to extend the line of separation. It is also striking that with the application of the synthetic jet, the flow around the sting support was significantly improved or streamlined, a finding that has promising implications in reducing or eliminating interference drag. The results are summarised in Table 2.

With no synthetic jet applied, the flow separation line was reasonably constant over the sphere surface. With the actuation of the synthetic jet, however, an asymmetrical flow field was generated which improved the flow by delaying separation three-dimensionally over the sphere. Interestingly, as previously mentioned, the synthetic jet was able to delay flow separation in the region of interference from the sting support more so than at the free end. With the section around port 2 the improvement was twice as that of port 4, approximately by 40% as opposed to nearly 20% (Table 2).

The flow over the sphere, even with the actuation of the synthetic jet and a side-mounted sting support, remained in the laminar flow regime as evidenced by the pressure distribution. Thus, the present synthetic jet strength and frequency of actuation did not trip the flow regime into turbulent flow.

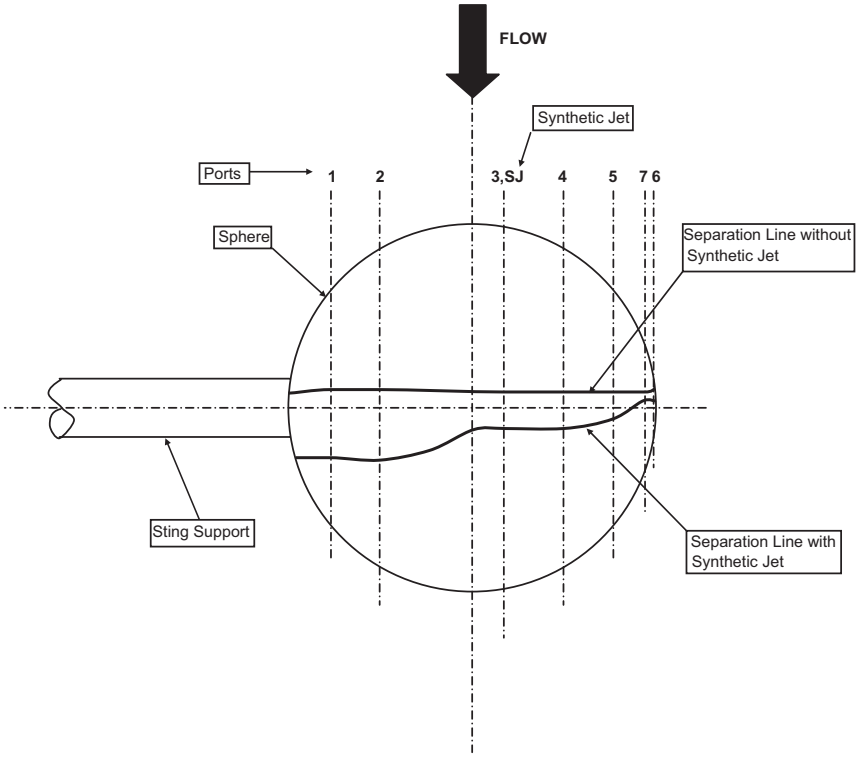

Fig. 9. Top view. Diagrammatic representation of separation with and without synthetic jet.

Table 2
Angles of flow separation

Port no.	Port location (γ)	Angle of separation (no synthetic jet)	Angle of separation (synthetic jet)	Improvement (%)
1	50	85	115	35.3
2	30	84	117	39.3
3	−10	82	101	23.2
4	−30	82	99	20.7
5	−50	83	93	12.0
7	−70	83	82	−1.2
6	-80	82	83	1.2

Table 3
Sectional drag coefficients

Drag analysis				
Port no.	Port location (γ)	C_d (no synthetic jet)	C_d (synthetic jet)	Reduction in C_d (ΔC_d) (%)
1	50	0.0487	0.0314	35.4
2	30	0.2708	0.2378	12.2
3	−10	0.4380	0.4029	8.0
4	−30	0.1991	0.1607	19.3
5	−50	−0.0101	−0.0322	219.5
7	−70	0.0134	0.0102	23.8
6	−80	0.0018	0.0001	95.3

3.6. A comparison of the coefficient of drag on the sphere

The sectional drag, defined in the usual sense as the drag acting on a section or on a particular plane of the body, was examined as circumscribed by each of the pressure ports on the sphere using the relationship given by

$$C_D = \int_0^{\pi} C_p \sin(2\phi)\, \mathrm{d}\phi. \tag{5}$$

Although it does not account for the skin friction drag, it provides a reasonable estimate of the drag on the sphere since form drag is the major contributor to the total drag at this Reynolds number.

The values of the coefficient of sectional drag are listed in Table 3 as well as the improvement for each section.

The three-dimensional drag coefficient of the sphere was calculated by integrating each of the sectional drag coefficients using the "matlab" software. The drag on the sphere without the application of the synthetic jet was 0.491. This compares favourably with the coefficient of drag, $C_D = 0.485$ given by Schlichting (1968). The total drag with the application of the synthetic jet was 0.431. This gives a total reduction in drag due to the actuation of the localised asymmetric synthetic jet of slightly over 12%. Table 3 shows the effect of the sting support, which is generating more drag on the side of the sphere it is attached to than the free side, as would be expected. Also of interest is port 5 which, at this section of the sphere, the asymmetric flow field seems to have created such a great reduction in drag, especially with the synthetic jet applied, that it produces a lift force on the sphere. This was also pointed out in the flow visualisation study that showed the tufts were strongly influenced across the sphere surface towards the sting support. Although there is a lift force opposing the drag on this section of the sphere and there is an immense improvement of nearly 220%, it contributes slightly less than 5% to the overall reduction in drag.

4. Concluding remarks

The present study has shown some notable effects of a synthetic jet and its impact on the flow over a true three-dimensional bluff body.

The study suggests of a critical angle of 27°, below which the effects of synthetic jet on the flow over a sphere become ineffective. The limitations of the potential flow theory beyond this critical angle, where the growth of the boundary layer becomes more pronounced, were also demonstrated. The deviation from potential flow theory increased as the angle offset increased, as expected.

The aerodynamic improvement owing to the asymmetric localisation of the synthetic jet was manifest in the delay of separation of flow that was found to range the angles of 83°–120° at a Reynolds number of 5×10^4. Additionally, the synthetic jet generated significant reductions to the total drag on the sphere with an overall reduction of over 12%.

The sting support had the effect of disturbing the flow upstream and downstream in its near vicinity. The downstream effects were observed from the flow visualisation study, which showed the flow from the sphere wake combining with the wake from the sting support, forming an asymmetrical interference type of flow. Fluid from the opposite side of the sting support was tending towards the sting at angles beyond 90°. The actuation of the synthetic jet lessened the asymmetric effect of the sting and improved the flow. This indicated that synthetic jets were capable of not only improving the flow on two-dimensional bodies but also streamlining the flow on three-dimensional bluff bodies with the added complexity of flow disturbances from interference effects. The pressure distribution plots provided further qualitative and quantitative evidence.

Significant drag reductions were also observed at certain points away from the synthetic jet but with generally smaller contribution to the overall drag of the sphere. Thus, activation of the asymmetric localised synthetic jet provided a technique to substantially improve the aerodynamic drag of the sphere.

The above findings will have significance beyond those envisioned in this study. Apart from localised synthetic jet used as an effective tool for aero-shaping true three-dimensional bluff and lifting bodies, the use of localised synthetic jet will also have significance of practical importance in various fluid mechanical devices and in industries where control of three-dimensional flow separation and re-attachment and streamlining of flows is required.

Acknowledgements

The authors would like to thank The Australian Research Council and CSR Edmonds for providing funding to the project, and Terry Flynn, the technical officer in charge of the UNSW aerodynamics laboratory, for his assistance during the conduct of the experimental work.

References

Ahmed, N.A., Archer, R.D., 2001. Post-stall behaviour of a wing under externally imposed sound. AIAA Journal of Aircraft 38 (5), 961–963.

Ahmed, N.A., Wagner, D.J., 2003. Vortex shedding and transition frequencies associated with flow around a circular cylinder. AIAA Journal 41 (3), 542–548.

Amitay, M., Kibens, V., Parekh, D.E., Glezer, A., 1999. Flow reattachment dynamics over a thick airfoil controlled by synthetic jet actuators. In: 37th AIAA Aerospace Sciences Meeting, Reno, Nevada, USA, pp. 99–1001.

Amitay, M., Smith, D.R., Kibens, V., Parekh, D.E., Glezer, A., 2001. Aerodynamic flow control over an unconventional airfoil using synthetic jet actuators. AIAA Journal 39 (3), 361–370.

Anderson Jr., J.D., 2001. Fundamentals of Aerodynamics, third ed. McGraw Hill, New York.

Barlow, B.J., Rae Jr., W.H., Pope, A., 1999. Low-speed Wind Tunnel Testing, third ed. Wiley, New York.

Bradshaw, P., 1970. Experimental Fluid Mechanics, second ed. Pergarmon Press, New York.

Buresti, G., 2000. Bluff-body aerodynamics. In: Proceedings Wind-Excited and Aeroelastic Vibrations of Structures, Genoa, Italy, June 12–16.

Clift, R., Grace, J.R., Weber, M.E., 1978. Bubbles, Drops and Particles. Academic Press, New York.

Glezer, A., Amitay, M., 2002. Synthetic jets. Annual Review of Fluid Mechanics 34, 503–529.

Gogineni, S.P., Joslin, R.D., Gaitonde, D.V., 2003. Aerospace America. Aerospace Sciences, Fluid Dynamics, December.

Gorder, P.F., 2004. New Scientist, 23 October, pp. 30–34.

Jeon, S., Choi, J., Jeon, W., Choi, H., Park, J., 2004. Active control of flow over a sphere for drag reduction at a subcritical Reynolds number. Journal of Fluid Mechanics 517, 113–129.

Kim, H.J., Durbin, P.A., 1988. Observations of the frequencies in a sphere wake and of drag increase by acoustic excitation. Physics of Fluids 31, 3260–3265.

Lee, C.Y., Goldstein, D.B., 2000. Two-dimensional synthetic jet simulation. AIAA Fluids Meeting, Denver, Colorado, USA, 2000-0406.

Mittal, R., Rampunggoon, P., 2002. On the virtual aeroshaping effect of synthetic jets. Physics of Fluids 14 (4), 1533–1536.

Norberg, C., 2002. Fluctuating lift on a circular cylinder: review and new measurements. Journal of Fluids and Structures 17, 57–96.

Pisasle, A.J., Ahmed, N.A., 2002a. Theoretical calibration for highly three-dimensional low-speed flows of a five-hole probe. Measurement Science and Technology 13, 1100–1107.

Pisasle, A.J., Ahmed, N.A., 2002b. A novel method for extending the calibration range of five-hole probe for highly three-dimensional flows. Flow Measurement and Instrumentation 13, 23–30.

Pisasale, A.J., Ahmed, N.A., 2004. Development of a functional relationship between port pressures and flow properties for the calibration and application of multihole probes to highly three-dimensional flows. Experiments in Fluids 36 (3), 422–436.

Reshotko, E., 1976. Boundary-layer stability and transition. Annual Review of Fluid Mechanics 8, 311–349.

Saffman, P.G., 1992. Vortex Dynamics. Cambridge University Press, New York.

Schlichting, H., 1968. Boundary-Layer Theory, sixth ed. McGraw Hill, New York.

Smith, B.L., Glezer, A., 1998. The formation and evolution of synthetic jets. Physics of Fluids 10 (9), 2281–2297.

Taneda, S., 1978. Visual observations of the flow past a sphere at Reynolds numbers between 10^4 and 10^6. Journal of Fluid Mechanics 85, 187–192.